DOI: 10.61782/fa.2023.0928

forum acusticum 2023

TRANSDIMENSIONAL PARTICLE FILTERING FOR GEOACOUSTIC INVERSION APPLIED TO VERTICAL AND HORIZONTAL ARRAYS

WU Weiwen [1,2,3] **REN Qunyan** [1,2,3*] **LI He** [1,2,3] **MA Li** [1,2,3]
[1] Institute of Acoustics, Chinese Academy of Sciences,
University of Chinese Academy of Sciences, Beijing, China;
[2] Key Laboratory of Underwater Acoustic Environment,
Chinese Academy of Sciences, Beijing, China;
[3] Institute of Acoustics, Chinese Academy of Sciences,
Road West NO.21 of Beijing's North 4th Ring, 100190 Beijing, China

ABSTRACT

In this study, a transdimensional particle filtering method is proposed to simultaneously estimate a geoacoustic model and its associated parameters, whose computational efficiency is improved through a mechanism of parallel calculations. The proposed method is first applied to seabed bottom loss derived from vertical array data collected in the Yellow Sea in 2016. The thickness and number of estimated sediment layers are close to those obtained in previous studies. Moreover, particle filtering has an intrinsic advantage in sequential processing, making it a straightforward method for mapping range-dependent geoacoustic properties of a horizontal array towed from a moving ship. Range-dependent inversion is conducted for a spatial varying environment, and the data are collected from an experiment conducted in the South China Sea in 2022. The inversion results suggest that the sediment layer and associated geoacoustic parameters can be effectively tracked and that the thickness and number of estimated sediment layers are consistent with those obtained by reversible jump Markov chain Monte Carlo method.

Keywords: *geoacoustic inversion, ambient noise, ship self-noise, transdimensional particle filtering, model selection.*

1. INTRODUCTION

Various sonar applications, such as sonar performance prediction, require the information of sediment geoacoustic models and their associated parameters, which are generally acquired using inversion methods [1,2]. In geoacoustic inversion, the parameterization of a geoacoustic model is a critical step because it has a considerable influence on the accuracy of the estimated parameter values and associated uncertainties [3-6]. Underparameterized and overparameterized models generally lead to wrong uncertainty estimations. The joint estimation of a geoacoustic model and its associated parameters has been achieved through a reversible jump Markov chain Monte Carlo (rjMCMC) methodology [7]. In this study, a transdimensional particle filter (TDPF) method is proposed, which can perform model selection by adding a birth–death form to a traditional particle filter and can increase computation efficiency by calculating particle swarms in parallel [8,9].

The proposed method is first tested on seabed bottom loss (BL) data derived from ambient noise data recorded by a vertical line array (VLA). Moreover, The TDPF method is applied to the self-noise data of the ship collected from a towed horizontal line array (HLA) in the South China Sea to test its feasibility to map the range-dependent geoacoustic properties. For HLA data processing, the cross-spectral density matrix (CSDM) of sound pressure is used as the

*[*]**Corresponding author**: renqunyan@mail.ioa.ac.cn*

observation data and the effectiveness and accuracy of the proposed method are evaluated.

2. TRANSDIMENSIONAL PARTICLE FILTER

The inference process of geoacoustic inversion, which involves sediment properties that exhibit spatial variations, must account for structural changes in the layering, such as alterations in the number of layers across the desired depth range. Consequently, when performing sequential inversion, the number of unknown parameters should be regarded as variable, and the posterior probability distributions (PPDs) of these parameters can encompass multiple parameter spaces characterized by different dimensions.

Let $d \in \mathbf{R}^N$ be a random variable containing N observed data. Let $\boldsymbol{I}_k$ be a set of models, where $k \in K$, and K is a countable set and k is the model index. Let $\mathbf{m}_k \in \mathbf{R}^{M_k}$ be a parameter vector of the model $\boldsymbol{I}_k$, where M_k is the parameter number in parameter vectors. The posterior probability distributions for k and $\mathbf{m}_k$ can be expressed as

$$P(k,\mathbf{m}_k \mid \mathbf{d}) = \frac{P(k)P(\mathbf{d} \mid k,\mathbf{m}_k)P(\mathbf{m}_k \mid k)}{\sum_{k' \in K}\int_M P(k')P(\mathbf{d} \mid k',\mathbf{m}'_{k'})P(\mathbf{m}'_{k'} \mid k')d\mathbf{m}'_{k'}}, \tag{1}$$

where $P(k)$ is the prior probability of the model k. The joint likelihood function of J frequencies is given by

$$P(\boldsymbol{d} \mid k,\boldsymbol{m}_k) = \prod_{j=1}^{J}\left\{\frac{N}{\pi V(f_j)\mathrm{Tr}[\mathbf{R}(f_j)]}\exp\left[-\frac{B(f_j,\boldsymbol{m}_k)}{V(f_j)}\right]\right\}^N, \tag{2}$$

where $\mathbf{R}(f_j) = \mathbf{d}(f_j)\mathbf{d}^{\mathrm{H}}(f_j)$ denotes the CSDM, $\mathbf{d}(f_j)$ denotes the acoustic pressure data. $B(f_j,\boldsymbol{m}_k)$ denotes the normalized Bartlett mismatch, expressed as

$$B(f_j,\boldsymbol{m}_k) = \frac{1-\mathbf{d}^H(f_j,\boldsymbol{m}_k)\mathbf{R}(f_j)\mathbf{d}(f_j,\boldsymbol{m}_k)}{(\|\mathbf{d}(f_j,\boldsymbol{m}_k)\|^2\ \mathrm{Tr}[\mathbf{R}(f_j)])}. \tag{3}$$

The normalized data error variance $V(f_j)$ can be expressed as

$$V(f_j) = B(f_j,\boldsymbol{m}_k), \tag{4}$$

where $\boldsymbol{m}_k$ is the optimal estimate of the parameter vector. The N in Eq. (2) is generally replaced with the effective number of propagation modes N_e.

Due to the high computational cost associated with estimating evidence for all relevant models, a commonly employed strategy is to use a uniform prior distribution for the models; that is, for all models,

$$P(k) = P(k'). \tag{5}$$

Hence, the denominator of Eq. (1) is $P(k')\sum_{k' \in K} P(\mathbf{d} \mid k')$.

After simplification, Eq. (1) can be rewritten as

$$P(k,\mathbf{m}_k \mid \mathbf{d}) = \frac{P(\mathbf{d} \mid k,\mathbf{m}_k)P(\mathbf{m}_k \mid k)}{\sum_{k' \in K} P(\mathbf{d} \mid k')}. \tag{6}$$

Let $\mathbf{X}' = \{k,\mathbf{m}_k\}$. In sequential Bayesian Monte Carlo method,

$$P(\mathbf{X}'_{0:t} \mid \mathbf{d}_{1:t}) \approx \sum_{i=1}^{N_P}\omega_t^{(i)}\delta(\mathbf{X}'_{1:t} - \mathbf{X}'^{(i)}_{1:t}). \tag{7}$$

where t is the time index, and the importance weights can be written recursively as

$$\omega_t^{(i)} = \omega_{t-1}^{(i)}\frac{P(\mathbf{d}_t \mid \mathbf{X}'^{(i)}_t)P(\mathbf{X}'^{(i)}_t \mid \mathbf{X}'^{(i)}_{t-1})}{\pi(\mathbf{X}'^{(i)}_t \mid \mathbf{X}'^{(i)}_{0:t-1},\mathbf{d}_{1:t})}. \tag{8}$$

Using the prior distribution as the important distribution yields in a particular case, the importance sampling function can be recursively written as

$$\pi(\mathbf{X}'_{0:t} \mid \mathbf{d}_{1:t}) = P(\mathbf{X}'_{0:t}) = P(\mathbf{X}'_0)\prod_{t'=1}^{t}P(\mathbf{X}'_{t'} \mid \mathbf{X}'_{t'-1}). \tag{9}$$

Hence, the importance weight for particle i can be rewritten as

$$\omega_t^{(i)} = \omega_{t-1}^{(i)} P(\mathbf{d}_t \mid \mathbf{X}_t^{'(i)}) . \tag{10}$$

If $P(\mathbf{X}_t^{'} \mid \mathbf{X}_{t-1}^{'})$ is given, accounting for the model in TDPF is feasible. Assuming that k and $\mathbf{m}_k$ are independent. $P(\mathbf{X}_t^{'} \mid \mathbf{X}_{t-1}^{'})$ can be expressed as

$$P(\mathbf{X}_t^{'} \mid \mathbf{X}_{t-1}^{'}) = P(\mathbf{m}_{k_{t-1}}^{'}, k_t \mid \mathbf{m}_{k_{t-1}}, k_{t-1}) P(\mathbf{m}_{k_t}, k_t \mid \mathbf{m}_{k_{t-1}}^{'}, k_t). \tag{11}$$

The uniform prior distribution is used in this paper. Hence,

$$P(\mathbf{m}_k \mid k) = \prod_{i=1}^{N_1} \Delta\eta_i \left(\prod_{i=1}^{N_2} \Delta\gamma_i \right)^k , \tag{12}$$

where N_1 is the dimension of the nongeoacoustic parameters, N_2 is the dimension of the geoacoustic parameters for one layer, $\Delta\eta_i$ is the width of the prior distribution of the parameter η_i, and $\Delta\gamma_i$ is the width of the prior distribution of the parameter γ_i. For all models, $P(k) = P(k^{'})$. Therefore,

$$\frac{P(k, \mathbf{m}_k)}{P(k^{'}, \mathbf{m}_{k^{'}})} = \frac{P(\mathbf{m}_k \mid k)}{P(\mathbf{m}_{k^{'}} \mid k^{'})} = \frac{\left(\prod_{i=1}^{N_2} \Delta\gamma_i \right)^k}{\left(\prod_{i=1}^{N_2} \Delta\gamma_i \right)^{k^{'}}} . \tag{13}$$

A birth–death form of models is added, which allows model selection. The birth–death rule is as follows:

(1) Birth: The number of layers is increased by 1. A random depth is selected in $[h_0, h_{\max}]$ as the new layer interface, where h_0 denotes the minimum depth of sediment, $h_{\max}$ denotes the maximum depth of sediment. The geoacoustic parameters of one of the layers are disturbed. Subsequently, all parameters are perturbed using a Gaussian proposal distribution.

(2) Death: A random layer interface is selected and deleted from the model. The geoacoustic parameters of the new layer are the same as one of the two original layers. Subsequently, all parameters are perturbed using a Gaussian proposal distribution.

(3) Perturb: The number of layers is constant. Furthermore, all parameters are perturbed using a Gaussian proposal distribution.

All three move types are assigned a probability of 1/3. If $P(\mathbf{X}_t^{'} \mid \mathbf{X}_{t-1}^{'})$ is given, it is feasible to take the model into account in a particle filter. For a birth move,

$$P(\mathbf{m}_{k_{t-1}}^{'}, k_t \mid \mathbf{m}_{k_{t-1}}, k_{t-1}) = \left(\prod_{i=1}^{N_2} \Delta\gamma_i \right)^{-1} , \tag{14}$$

$$P(\mathbf{m}_{k_t}, k_t \mid \mathbf{m}_{k_{t-1}}^{'}, k_t) = [(2\pi)^{L_{\mathbf{m}_{k_t}}} \mid \mathbf{C} \mid]^{-1/2} \times \exp[-\frac{1}{2}(\mathbf{m}_{k_t} - \mathbf{m}_{k_{t-1}}^{'})^{\mathrm{T}} \mathbf{C}^{-1} (\mathbf{m}_{k_t} - \mathbf{m}_{k_{t-1}}^{'})] , \tag{15}$$

where $L_{\mathbf{m}_{k_t}}$ denotes the dimension of $\mathbf{m}_k$, and $\mathbf{C}$ denotes the covariance matrix of the Gaussian proposal. Hence, $P(\mathbf{X}_t^{'} \mid \mathbf{X}_{t-1}^{'})$ can be expressed as follows:

$$P(\mathbf{X}_t^{'} \mid \mathbf{X}_{t-1}^{'}) = \left(\prod_{i=1}^{N_2} \Delta\gamma_i \right)^{-1} [(2\pi)^{L_{\mathbf{m}_{k_t}}} \mid \mathbf{C} \mid]^{-1/2} \times \exp[-\frac{1}{2}(\mathbf{m}_{k_t} - \mathbf{m}_{k_{t-1}}^{'})^{\mathrm{T}} \mathbf{C}^{-1} (\mathbf{m}_{k_t} - \mathbf{m}_{k_{t-1}}^{'})] . \tag{16}$$

For a death move, $P(\mathbf{X}_t^{'} \mid \mathbf{X}_{t-1}^{'})$ can be expressed as follows:

$$P(\mathbf{X}_t^{'} \mid \mathbf{X}_{t-1}^{'}) = \left(\prod_{i=1}^{N_2} \Delta\gamma_i \right)^{1} [(2\pi)^{L_{\mathbf{m}_{k_t}}} \mid \mathbf{C} \mid]^{-1/2} \times \exp[-\frac{1}{2}(\mathbf{m}_{k_t} - \mathbf{m}_{k_{t-1}}^{'})^{\mathrm{T}} \mathbf{C}^{-1} (\mathbf{m}_{k_t} - \mathbf{m}_{k_{t-1}}^{'})] . \tag{17}$$

For a perturb move, $P(\mathbf{X}_t^{'} \mid \mathbf{X}_{t-1}^{'})$ can be expressed as follows:

$$P(\mathbf{X}_t^{'} \mid \mathbf{X}_{t-1}^{'}) = [(2\pi)^{L_{\mathbf{m}_{k_t}}} \mid \mathbf{C} \mid]^{-1/2} \times \exp[-\frac{1}{2}(\mathbf{m}_{k_t} - \mathbf{m}_{k_{t-1}}^{'})^{\mathrm{T}} \mathbf{C}^{-1} (\mathbf{m}_{k_t} - \mathbf{m}_{k_{t-1}}^{'})] . \tag{18}$$

The algorithm flow is shown in Fig. 1. Several iterations for every time t can improve the accuracy of parameter estimation. The iteration step is not shown in Fig. 1.

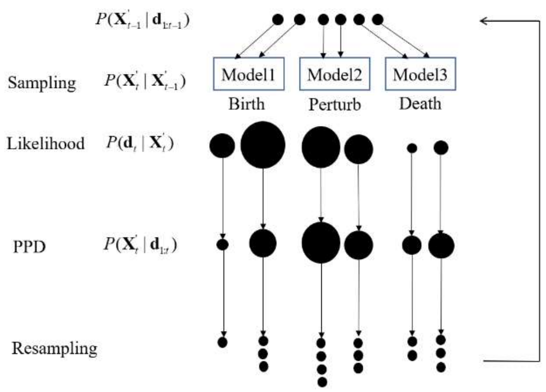

Figure 1. Algorithm flow of TDPF method. The particles have an equal probability of selecting model 1 (birth), model 2 (perturb), or model 3 (death). The black circles represent the probability magnitude.

3. GEOACOUSTIC INVERSION USING AMBIENT NOISE

Various information about the seabed, such as the sediment layering numbers and geoacoustic parameters, considerably affect the spatial distribution of ambient noise. The ambient noise received by the VLA can be used to calculate the wideband seabed BL, which is used as the input data of the TDPF to estimate the sediment layering structure and associated geoacoustic parameters.

The experimental data were collected in the Yellow Sea of China, December 2016, where the water depth is ~35 m. The frequency range is 1000–3700 Hz, and 28 frequency points are selected at an even frequency interval. A 25-element VLA with an equal interval of 0.2 m was used to collect ambient noise data. The OASN [10] is used here to calculate the replica ambient noise pressure field, and the BL extraction method is based on Harrison's theory [11]. The extracted BL model is shown in Fig. 2. In TDPF, the particle number is 2000 for each iteration. To ensure convergence, a conservative choice of 5 iterations is selected, acknowledging that it may be a relatively large number. Subsequent inversion results indicate that the number of sedimentary layers and the distribution of parameters are basically unchanged during the last 3 iterations.

The estimated number of sediment layers (including the basement) changing with TDPF iterations is shown in Fig. 3. The inversion results obtained using TDPF method indicate that there is a sediment layer of the seafloor in this area. The interface probability and marginal posterior probability profiles for the seabed sound speed are shown in Fig. 4. The Posterior probability densities (PPDs) of the parameters show that the peak value of the thickness of the sediment layer (h) is 0.94 m, the sound velocity of the sediment layer (c_1) is 1531 m/s, and the sound velocity of the basement (c_2) is 1635 m/s. The inversion results for this area are consistent with those reported in previous studies [12,13], where the sound velocity of the sediment layer is 1535 m/s and the thickness of the sediment layer is 1.1 m.

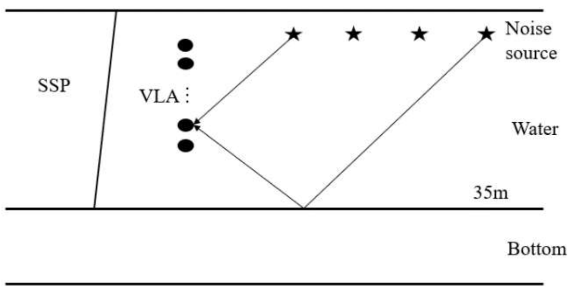

Figure 2. Experimental configuration for bottom loss extraction.

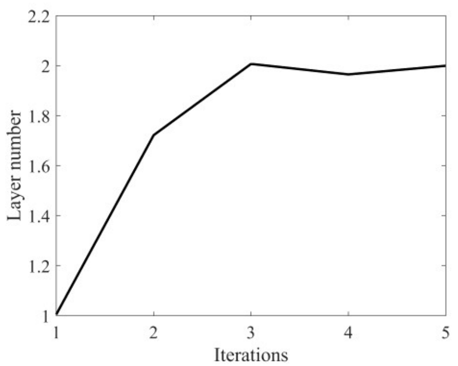

Figure 3. Changes in the number of layers with PF iterations.

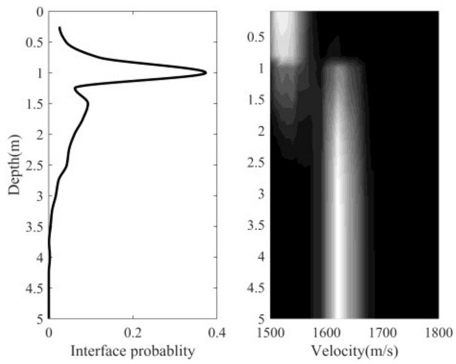

Figure 4. Interface probability and marginal posterior probability profiles for seabed sound speed. The solid line in the left represents the layered PPD. In the right, the brighter areas indicate higher PPDs. (The same bellow)

The BL computed from particles in the last iteration and the BL computed from trial data are shown in Fig. 5. The trends and turning points of the two are roughly consistent, and the fitting performance of the BL is good for grazing angles above 40 degrees. However, the fitting performance of the BL for grazing angles below 40 degrees is not very well, which may be caused by ship noise interference.

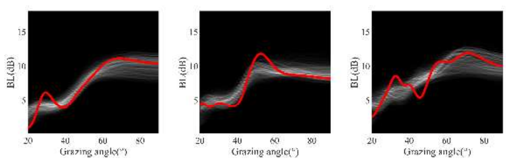

Figure 5. BL fitting diagrams at 1300, 1800, 2300 Hz respectively. The solid line represents the BL calculated from the trial data, and the brightness represents the value of PPDs, with brighter areas indicating higher PPDs.

4. GEOACOUSTIC INVERSION USING SHIP SELF-NOISE

The TDPF method is a promising approach for dealing with range-dependent inversion. It has an intrinsic advantage in sequential processing compared to rjMCMC. In the rjMCMC method, each Markov chain needs to calculate samples one by one to decide whether to accept new samples. In contrast, the TDPF method can simultaneously calculate the weights of all particles for one iteration. This enables TDPF to efficiently utilize computational resources by employing batch processing instead of individual sampling, and it achieves approximate posterior distributions similar to rjMCMC.

The TDPF method is applied to the ship self-noise data collected by the HLA for a range-dependent environment. The self-noise data were collected in September 2022 in the South China Sea, and the source ship was Experiment Research Ship No. 1, a large catamaran with a draught depth of 6 m. The sound sources used in this study are three line spectra of 141.75, 145.25, and 723.5 Hz, and the depth of the self-noise source of the ship is ~5.0 m. According to the cable length, the source range is 250–300 m. The interval of 64 elements of the HLA is 1.5 m, the depth of the HLA is ~44 m, and the water depth measured by the echo sounder is ~107 m. The number of sediment layers is unknown. The Hamilton empirical formula [14] between sound velocity and density is used here. The parameters involved in inversion are as follows: source depth SD, source range R, array length L, array depth RD, water depth WD, sediment layering numbers, sediment layering thickness, sediment layering sound velocity, and basement sound velocity. In TDPF, the particle number is 5000 for each iteration. The vertical array data indicates that convergence has been basically achieved after 3 iterations. The parameter information contained in the consecutive data segments of horizontal array data is similar, implying abundant prior information compared to the vertical array. Furthermore, the particle number for each iteration is 2.5 times than that in section 3. Therefore, a choice of 3 iterations is selected in this case. Subsequent inversion results indicate that the number of sedimentary layers and the distribution of parameters are basically unchanged after 2 iterations. The first two iterations are used to select the number of sediment layers and N_e is selected as 6. The last iteration is used to estimate the uncertainty of parameters and enhance particle diversity, in which the likelihood function is flatter compared to the first two iterations by decreasing N_e. The collected data are split into 20 data segments, and the length of each data segment is 30 s.

The tracking results of the parameters of TDPF are shown in Fig. 6. The number of sediment layers obtained via TDPF inversion in this experiment is 2; the thickness of the sediment layer is denoted as h and the sound velocity of sediment and basement are denoted as c_1 and c_2, respectively. Figure 7 shows that the layer number of sediment is almost 2 for each data segment. The estimated layer number and sediment thickness are consistent with those the echo sounder. Figure 8 shows the inversion results of the geoacoustic model and associated velocity for data segment No. 3. The inversion results obtained by rjMCMC are shown in Fig. 9. The Markov chain number is 1 and 5000 samples are used here. The nongeoacoustic parameters are estimated from traditional particle filter and fixed, while the geoacoustic model and parameters are variable in rjMCMC. The TDPF and rjMCMC obtain similar inversion results. Because the source level of the ship's noise is unknown, it is impossible to calculate the exact transmission loss (TL) value; only the TL trend of power spectral density (PSD) can be obtained. The calculated TL using inversion results of the fourth frame and the PSD of data segment No. 3 are shown in Fig. 10. Comparing the lines, the TL trends are consistent, indicating that the inversion results are reliable.

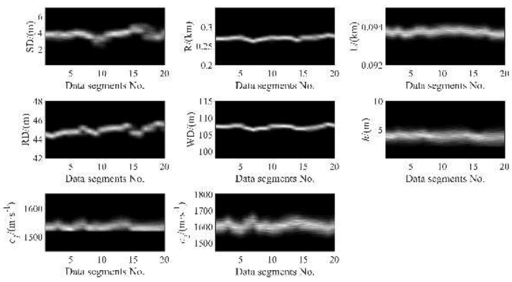

Figure 6. PPDs of parameters for 20 data segments.

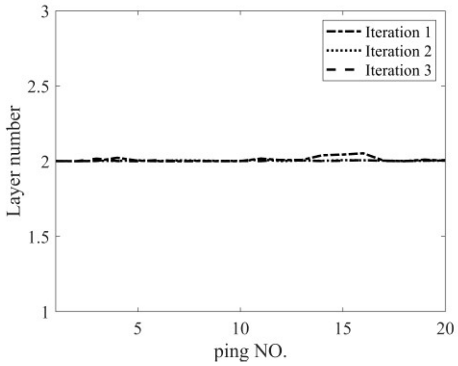

Figure 7. Changes in the number of layers with iteration.

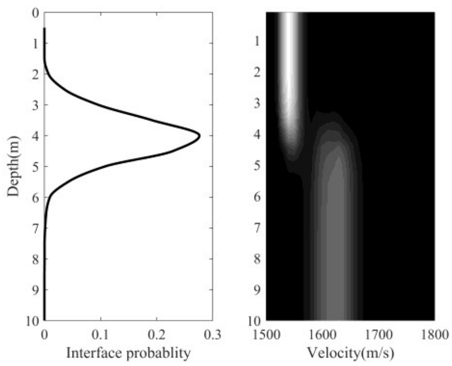

Figure 8. PPD of interface probability and velocity of data segment No.3 (TDPF).

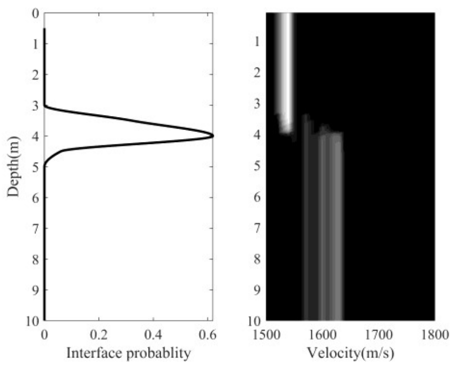

Figure 9. PPD of interface probability and velocity of data segment No.3 (rjMCMC).

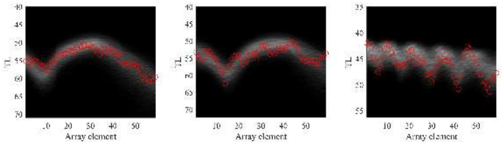

Figure 10. TL fitting diagrams of three frequencies of data segment No. 3. The dots indicate PSD, and the three images are for 141.75, 145.25, and 723.5 Hz, respectively, from left to right.

5. CONCLUSION

In this study, the proposed TDPF method is applied to ambient noise data collected by a VLA and ship self-noise data collected by a towed HLA to estimate parameters without model information. The inversion results show that the TDPF method can parameterize the geoacoustic model and estimate associated geoacoustic parameters. For inversion using ambient noise, the results of TDPF for BL data are consistent with previous studies. The intrinsic advantage of TDPF in sequential processing makes it suitable for range-dependent inversion. For inversion using ship self-noise, the predicted TL along the array fitted the PSD data well. The results show that the TDPF method is a promising method for geoacoustic inversion in range-dependent environments.

6. REFERENCES

[1] Dosso, S. E., Yeremy, M. L., Ozard, J. M., and Chapman, N. R. "Estimation of ocean-bottom properties by matched-field inversion of acoustic field data." IEEE Journal of Oceanic Engineering 18.3 (1993): 232-239.

[2] Gerstoft, P., and Mecklenbräuker, C. F. "Ocean acoustic inversion with estimation of a posteriori probability distributions." The Journal of the Acoustical Society of America 104.2 (1998): 808-819.

[3] Dosso, S. E. "Quantifying uncertainty in geoacoustic inversion. I. A fast Gibbs sampler approach." *The Journal of the Acoustical Society of America* 111.1 (2002): 129-142.

[4] Dosso, S. E. , and P. L. Nielsen . "Quantifying uncertainty in geoacoustic inversion. II. Application to broadband, shallow-water data." *The Journal of the Acoustical Society of America* 111.1 (2002): 143-159.

[5] Dettmer, J. , S. E. Dosso , and C. W. Holland . "Model selection and Bayesian inference for high-resolution seabed reflection inversion." *The Journal of the Acoustical Society of America* 125.2(2009):706-716.

[6] Battle, D. J., Gerstoft, P., Hodgkiss, W. S., Kuperman, W. A., and Nielsen, P. L. "Bayesian model selection applied to self-noise geoacoustic inversion." *The Journal of the Acoustical Society of America* 116.4(2004):2043-2056.

[7] Dettmer, J. , S. E. Dosso , and C. W. Holland . "Trans-dimensional geoacoustic inversion." *The Journal of the Acoustical Society of America* 128.6 (2010): 3393-3405.

[8] Bo, Liankun , J. Xiong , and S. Ma . "Sequential inversion of self-noise using adaptive particle filter in shallow water." *The Journal of the Acoustical Society of America* 143.4(2018):2487-2500

[9] Dettmer, Jan , S. E. Dosso , and C. W. Holland . "Sequential trans-dimensional Monte Carlo for range-dependent geoacoustic inversion." *The Journal of the Acoustical Society of America* 129.4(2011):1794-1806.

[10] Schmidt, H. 2004 OASES version 3.1 User Guide and Reference Manual (Cambridge, MA: Massachusetts Institute of Technology)

[11] Harrison, C. H., and Simons, D. G. "Geoacoustic inversion of ambient noise: a simple method. " *The Journal of the Acoustical Society of America* (2002).

[12] He, L., Xin-Yi, G., and Li, M. "Estimating structure and geoacoustic parameters of sub-bottom by using spatial characteristics of ocean ambient noise in shallow water." *Acta Physica Sinica* 68.21(2019).

[13] He, L. Extracting the Geoacoustic Parameters Passively Using the Spatial Characteristics of Ocean Ambient Noise in Shallow Water. *Ph.D. thesis*, University of Chinese Academy of Sciences, Institute of Acoustics, Chinese Academy of Sciences, 2021, pp. 85-89.

[14] Hamilton, E. L., and Bachman, R. T. "Sound velocity and related properties of marine sediments." The Journal of the Acoustical Society of America 72.6 (1982): 1891-1904.